Modulation of the Transient Receptor Potential Vanilloid Channel TRPV4 by 4α-Phorbol Esters: A Structure−Activity Study

Thomas Kjær Klausen,[†,§] Alberto Pagani,[‡] Alberto Minassi,[‡] Abdellah Ech-Chahad,[‡] Jean Prenen,[†] Grzegorz Owsianik,[†] Else Kay Hoffmann,[§] Stine Falsig Pedersen,[§] Giovanni Appendino,*[,‡] and Bernd Nilius*[,†]

KU Leuven, Department of Molecular Cell Biology, Laboratory Ion Channel Research, Campus Gasthuisberg, Herestraat 49, bus 802, Leuven, Belgium, Dipartimento di Scienze Chimiche, Alimentari, Farmaceutiche e Farmacologiche, Via Bovio 9, 28100 Novara, Italy, Department of Biology, Section of Cell and Developmental Biology, University of Copenhagen, 13 Universitetsparken, 2100 Copenhagen Ø, Denmark

Received October 24, 2008

The mechanism of activation of the transient receptor potential vanilloid 4 (TRPV4) channel by 4α-phorbol esters was investigated by combining information from chemical modification of 4α-phorbol-didecanoate (4α-PDD, **2a**), site-directed mutagenesis, Ca^{2+} imaging, and electrophysiology. Binding of 4α-phorbol esters occurs in a loop in the TM3−TM4 domain of TRPV4 that is analogous to the capsaicin binding site of TRPV1, and the ester decoration of ring C and the A,B ring junction are critical for activity. The lipophilic ester groups on ring C serve mainly as a steering element, affecting the orientation of the diterpenoid core into the ligand binding pocket, while the nature of the A,B ring junction plays an essential role in the Ca^{2+}-dependence of the TRPV4 response. Taken together, our results show that 4α-phorbol is a useful template to investigate the molecular details of TRPV4 activation by small molecules and obtain information for the rational design of structurally simpler ligands for this ion channel.

Introduction

The transient receptor potential (TRP[a]) channel proteins form cation-permeable structures of low evolutionary relation, grouped into seven subfamilies structurally characterized by six transmembrane (TM) domains and a pore region between TM5 and TM6.[1−5] Most TRP channels are Ca^{2+} permeable and sense multiple physical stimuli (cold, heat, osmolarity, voltage) as well as a plethora of noxious compounds and intracellular signaling molecules like endocannabinoids and phospholipase C (PLC)- and phospholipase A2 (PLA_2)-derived products.[1−5] Recently, evidence has been mounting that TRP channels, and especially those of the TRP vanilloid (TRPV)-type, are involved in a host of human inflammatory pathologies.[6] Thus, compounds capable of preventing activation of TRPV1 by classic receptor antagonism or by desensitization have been extensively investigated, and several capsaicinoid agonists and a host of synthetic TRPV1 antagonists have reached clinical studies.[7] The large number of TRPV1 ligands from the natural products pool has undoubtedly contributed to the wealth of studies on this channel, while much less is known regarding ligand interactions of related TRP channels (TRPV2−4).[8]

TRPV4 is widely expressed in epithelial cells and has also been found in the brain, endothelium, liver, and trachea.[9] Several lines of evidence have pointed out the involvement of TRPV4 in important pathological conditions such as hypotonic hyperalgesia, thermal hyperalgesia, asthma, and neuropathic pain.[10] Currently, the best described small molecule TRPV4 ligands are bisandrographolide A (BAA, **1**, Figure 1), a plant dimeric diterpenoid,[11] 4α-phorbol-12,13-didecanoate (4α-PDD, **2a**), a semisynthetic nontumor promoter phorbol ester,[12,13] and GSK1016790A (**3**), a synthetic peptide.[14,15] No recognized structural relationship exists between these compounds, and limited information is available on their structure−activity relationships. 4α-Phorbol esters have been extensively employed in biomedical research as negative controls for the activity of their corresponding phorbol esters, a class of ultrapotent biological analogues of the secondary messenger 2-arachidoylglycerol (2-AG) for the activation of protein kinase C (PKC).[16] The discovery that 4α-PDD (**2a**) strongly interacts with TRPV4 has further emphasized that the phorbol core, a per se biologically inert structure, is a pleiotropic framework for the induction of bioactivity by acylative modification.[17]

TRPV1 and TRPV4 show some degree of similarity (60% homology, 40% identity) in the TM3−4 region, an element involved in vanilloid binding and activation of TRPV1,[18] and site-directed mutagenesis experiments have indeed confirmed the location of a ligand-binding element in this region. Thus, mutation of L584A and of W586A in TM4 of TRPV4 specifically inhibited activation by heat and 4α-phorbol-esters,[19] while the mutations Y591A and R594A inhibited activation by all stimuli, suggesting a role in gating rather than in ligand binding.[13] The YS motif at the N-terminal end of TM3 in TRPV4 (Y556 and S557) is strongly reminiscent of the capsaicin domain of TRPV1,[20] and mutating Y556 to alanine strongly inhibited the activation of TRPV4 by 4α-phorbol-esters.[21] This effect correlated with the length of the aliphatic side chains of the 4α-phorbol esters, pointing to the involvement of Y556 in binding to the aliphatic side chain of these compounds.[13] Binding of 4α-phorbol-12-myristate-13-acetate (**2b**), an analogue of 4α-PDD (**2a**) with potent TRPV4 agonistic activity ($EC_{50} \sim 3\ \mu M$), was strongly affected by the Y556A mutation, while binding of 4α-phorbol diacetate (**2c**) was unaffected by this mutation,[19] suggesting that the long acyl moiety at C-12 is critically involved in binding. Conversely, mutation of S557 to

* To whom correspondence should be addressed. For B.N.: phone, +32 16 34 5937; fax, 32 16 34 5991; E-mail, bernd.nilius@med.kuleuven.be. For G.A.: phone, +39 0321375744; fax, +39 0321375621; E-mail, appendino@pharm.unipmn.it.

† KU Leuven, Department of Molecular Cell Biology, Laboratory Ion Channel Research.

§ Department of Biology, Section of Cell and Developmental Biology, University of Copenhagen.

‡ Dipartimento di Scienze Chimiche, Alimentari, Farmaceutiche e Farmacologiche.

[a] Abbrevations: TRP, transient receptor potential; TRPV, TRP vanilloid; TM, transmembrane; PLC, phospholipase C; PLA_2, phospholipase A2; PKC, protein kinase C; 2-AG, 2-arachidoylglycerol, NT, nontransfected.

10.1021/jm9001007 CCC: $40.75
Published on Web 04/10/2009

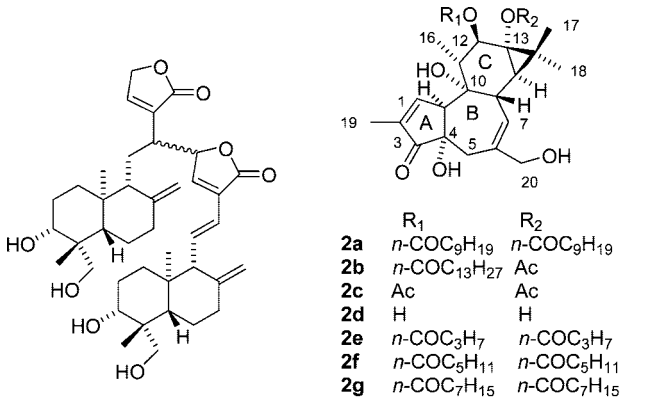

1

	R_1	R_2
2a	*n*-COC_9H_{19}	*n*-COC_9H_{19}
2b	*n*-$COC_{13}H_{27}$	Ac
2c	Ac	Ac
2d	H	H
2e	*n*-COC_3H_7	*n*-COC_3H_7
2f	*n*-COC_5H_{11}	*n*-COC_5H_{11}
2g	*n*-COC_7H_{15}	*n*-COC_7H_{15}
2h	*n*-COC_8H_{17}	*n*-COC_8H_{17}
2i	*n*-$COC_{13}H_{27}$	*n*-$COC_{13}H_{27}$
2j	*n*-$COC_{17}H_{35}$	*n*-$COCH_{17}H_{35}$
2k	H	*n*-COC_9H_{19}

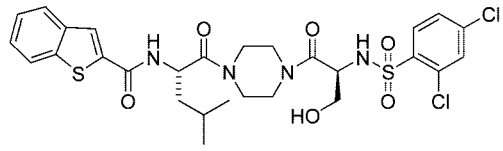

3

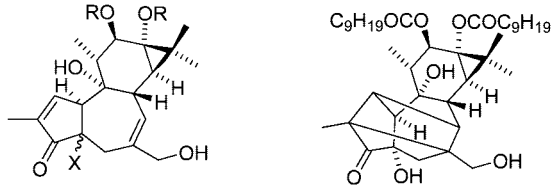

	X	R
4a	β-OH	H
4b	α-H	H
4c	α-H	*n*-COC_9H_{19}

5

Figure 1. Structural formulas of the TRPV4 ligands BAA (**1**), 4α-PDD (**2a**), GSK1016790A (**3**), of the new ligands investigated (**2e**−**k**, **4a**−**c**, and **5**), and of the reference phorboids **2b**−**d**.

alanine, a detrimental maneuver for capsaicin binding to TRPV1,[20] had little effect on 4α-PDD (**2a)** binding to TRPV4.[21]

Taken together, these data show that 4α-PDD (**2a**) is as an interesting template to investigate the molecular details of the interaction of TRPV4 with small molecules and obtain information for the rational design of structurally simpler synthetic analogues. For this purpose, we have focused on what have emerged as the two critical elements for the biological profile of 4α-PDD, namely the esterification pattern of ring C and the nature of the A,B rings and their junction.

Chemistry

Phorbol (**4a**) and 4-deoxy-4α-phorbol (**4b**) were obtained from commercial croton oil,[22] while 4α-phorbol (**2d**) was prepared from phorbol (**4a**) by base-catalyzed retro-aldol epimerization.[23] The reactivity pattern of the hydroxyls of phorbol is rather peculiar and is dominated by the surprisingly facile esterification of the tertiary C-13 hydroxyl and the easy removal of the allylic primary ester group at C-20.[22,24] The same pattern of reactivity was found in 4α-phorbol (**2d**) and in its 4-deoxyderivative (**4b**), whose acylative decoration, a critical element for TRPV4 binding,[19] could be varied by applying the protocols developed for phorbol esters.[22,24] Thus, by simply varying the amounts of acylating agent, 12,13,20-triesters and 13,20 diesters could be easily prepared from 4α-phorbol (**2d**, Scheme 1), while methanolysis of the primary allylic 20-ester groups eventually afforded the 12,13-diesters **2e**−**2j** and the 13-monoester **2k** from their corresponding triestes and the diesters.[24] In a similar way, the 4-deoxy analogue of 4α-PDD (**4c**) was obtained from 4α−4-deoxphorbol (**4b**), a byproduct from the isolation of phorbol from croton oil.[22] Finally, lumi-4α-PDD (**5**) was prepared from 4α-PDD by photochemical [$2\pi + 2\pi$] intramolecular photocycloaddition.[22]

Biological Evaluation

The activation of TRPV4 by 4α-phorbol deriviatives was evaluated by measuring their capacity to elicit an increase in the free intracellular Ca^{2+} concentration ($[Ca^{2+}]_i$) in mTRPV4 transfected HEK 293 cells, while electrophysiological studies were performed in the whole cell patch clamp mode. Because TRPV4 is activated by cell swelling, the osmolarity of this solution was changed by omitting mannitol from an isotonic solution (see Experimental Section).[19]

Results and Discussion

Ring C Acylation Pattern. Activity was strongly affected by the acylation pattern of the ring C hydroxyls. Within the series of esters investigated, the most potent compound was the 12,13-dihexanoate (**2f**) (4α-PDH, EC_{50} = 70 nM, Table 1, Figure 2). The closely related diacetate (**2c**), dioctanoate (**2g**), and dinonanoate (**2h**) showed only marginal activity at the maximal concentration assayed (50 μM), insufficient to estimate EC_{50} values (Table 1, Figure 2). On the other hand, while the 12,13-dimyristate (**2i**) showed decreased activity compared to 4α-PDD (**2a**), the 12,13-distearate (**2j**) turned out to be too lipophilic and insoluble to allow a reliable measurement of activity. These observations show that the relationship between the length of the side chain and the activity is not linear, with two maxima of activity at C-6 and C-10 carbon length, respectively. This differs markedly from the bell-shape curve of potency vs acyl moiety length observed for the activation of PKC by phorbol diesters.[16] A bell-shaped relationship also holds for the pungency of vanillamides, an indirect measurement of TRPV1 activation,[25] but this relationship is presumably more complex because the introduction of unsaturations has different effects in vanillamides with long (C-18) and medium (C9) length aliphatic chains, with a substantial dissociation of TRPV1 affinity and pungency.[25,26]

Previous site-selective mutagenesis data have suggested that the binding of 4α-phorbol-diesters to TRPV4-Y556 involves only the C-12 ester groups.[19] However, the diester 4α-PDD (**2a**) and its 13-monoester (**2k**) showed similar EC_{50} values (370 nM vs 450 nM, Table 1), although the maximal increase in $[Ca^{2+}]_i$ elicited, i.e., the efficacy, of the monoester (**2k**) was lower than that of the diester 4α-PDD (**2a**) (Figure 3). The relationship between location and length of the acyl moieties and TRPV4 activation by 4α-phorbol-esters is complex and better accommodated by a model of interaction where the ring C ester groups have an orienting- rather than a direct binding role, in contrast with a previous proposal.[19]

We next focused on the characterization of the TRPV4 response by the most potent compound of the series, 4α-PDH (**2f**) (EC_{50} value = 70 nM, Figure 4A). Given the poor activity of the dioctanoate **2g** and the dinonanoate **2h**, the almost 5-fold-higher potency of the dihexanoate **2f** compared to 4α-PDD **2a** raised the question whether the observed $[Ca^{2+}]_i$ increase indeed reflected TRPV4 activation. This was, however, clearly the case because: (i) **2f** did not affect $[Ca^{2+}]_i$ in nontransfected HEK293

Scheme 1. Synthesis of the 4α-Phorbol Diesters **2e**−**j**, the 4α-4-Deoxyphorbol Diester **4c**, and the 4α-Phorbol Ester **2k**

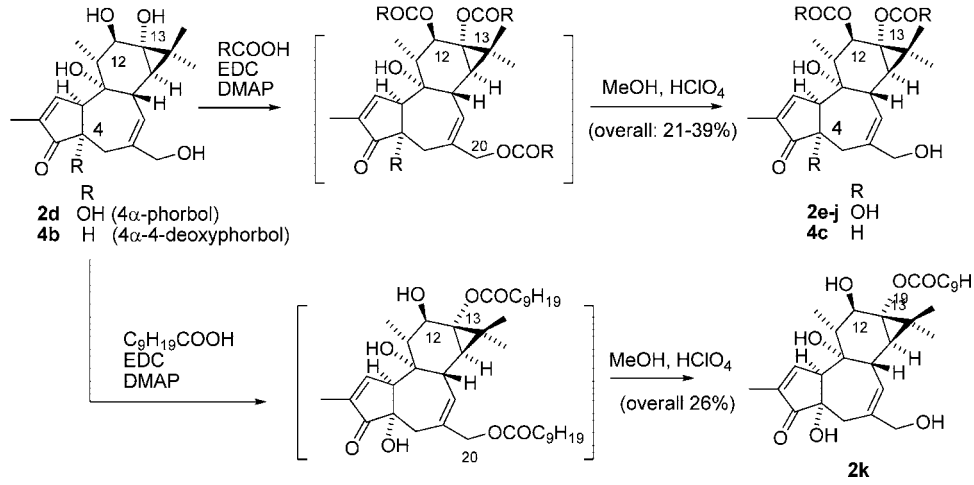

Table 1. Affinity Responses for Compounds **2a**,**c**,**e**−**k**, **4c**, and **5**[a]

			EC_{50} (μM)			
compd	carbons in acyl moiety	n_{Hill}	WT	Y556A	S557A	W586A
2a	10	2.2	0.37 ± 0.08	6.3*[b] ± 0.3	0.32 ± 0.15	>6*[b]
2c	2		>50			
2e	4	2.6	22.47 ± 4.04			
2f	6	1.5	0.07 ± 0.01	2.79 ± 1.15	0.36 ± 0.01	2.84 ± 1.12
2g	8		>50			
2h	9		>50			
2i	14	2.0	2.83 ± 0.62			
2j	18					
2k	10	2.0	0.45 ± 0.08			
4c	10		>50			
5	10	1.0	0.175 ± 0.07	9.36 ± 19.98	0.24 ± 0.20	3.64 ± 3.47

[a] EC_{50} values and Hill coefficients where calculated via eq 1 (See Experimental Section). [b] *Values taken from ref 19.

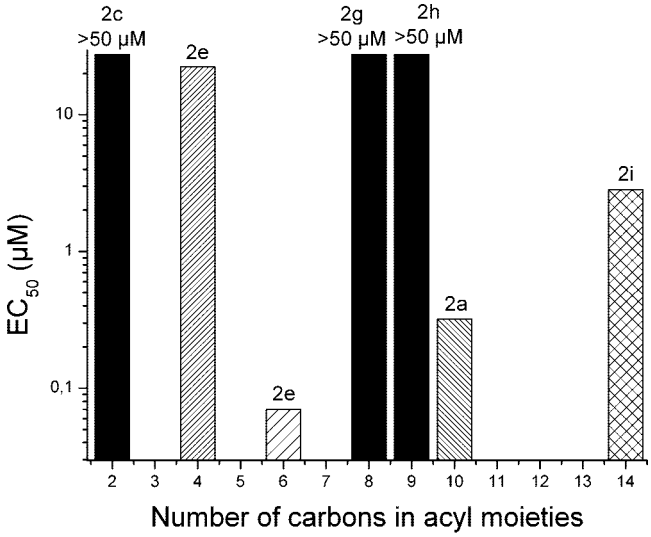

Figure 2. Relationship between EC_{50}values and side chain length of 4α-phorbol-diesters. EC_{50} values were calculated using eq 1. Results for each compound are based on >15 individual cells from at least three independent transfections.

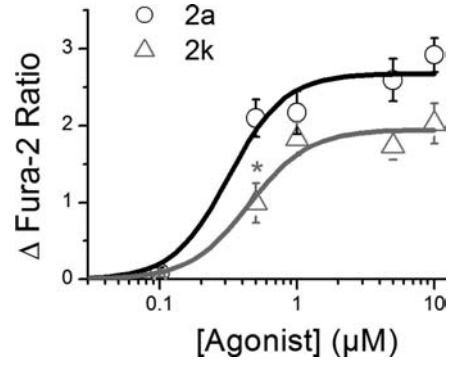

Figure 3. Comparison of the effects of 4α-PDD (**2a**) and the monoester 4α-PD (**2k**) on $[Ca^{2+}]_i$ in HEK293 cells. The relative increase in $[Ca^{2+}]_i$ (shown as the increase in 340/380 nm fura-2 fluorescence ratio after agonist addition, ΔFura-2 ratio) was estimated as a function of the bath concentration of 4α-PDD (**2a**, black circles) and 4α-PD (**2k**, gray triangles). Solid lines represent a fit to the Hill equation. Points are ΔFura-2 ratio for 18−32 individual cells from three independent transfections. * indicates significant differences at the level $p < 0.05$.

cells (data not shown), (ii) the response was dependent on extracellular Ca^{2+} (Figure 3B), and (iii) the increase in $[Ca^{2+}]_i$ was inhibited by the TRP antagonist ruthenium red (RR) (Figure 4C). In whole cell patch clamp studies of mTRPV4 transfected cells, **2f** activated currents with outward-inward rectification (Figure 5A) with less pronounced rectification in Ca^{2+} free solution (Figure 5B). The current could be reactivated, but exhibited substantial run-down, suggesting washout of an internal factor necessary for TRPV4 activation (Figure 5A,B).

Site directed mutagenesis has highlighted the relevance of residues L586, W586, and Y556 in 4α-phobol ester binding to TRPV4.[19] To assess whether **2f** activates TRPV4 by interaction with the same binding pocket as 4α-PDD (**2a**), dose−response experiments were performed on wild type, W586A, S557A, and Y556A mTRPV4 constructs expressed in HEK293 cells. Each mutation shifted the dose−response curves to higher concentrations, indicating that, indeed, **2f** activates TRPV4 by binding

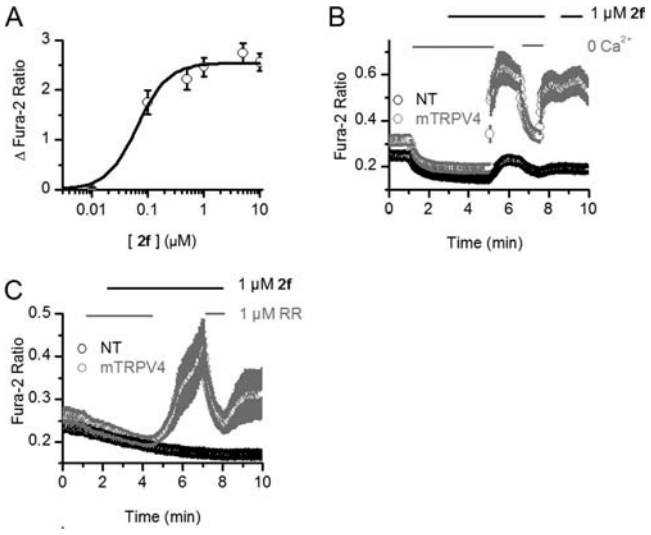

Figure 4. Effects of compound **2f** on $[Ca^{2+}]_i$in mTRPV4 transfected HEK 293 cells. (A) Dose−response relationship for **2f**. ΔFura-2 ratio was estimated by single cell Ca^{2+} imaging as described in the Experimental Section. Points are ΔFura-2 ratio estimated for 25−61 individual cells from three independent transfections. The solid line represents a fit to the Hill equation. (B) The response to **2f** is dependent on extracellular Ca^{2+}. Compound **2f** (1 μM) and extracellular Ca^{2+} were present as indicated by top bars. The figure is representative of three independent experiments for each condition and cell type. (C) The $[Ca^{2+}]_i$ response to **2f** (1 μM) is inhibited by ruthenium red (RR, 1 μM). The presence of RR and **2f** in the extracellular solution is indicated by the top bars. The figure is representative of three independent experiments for each condition and cell type.

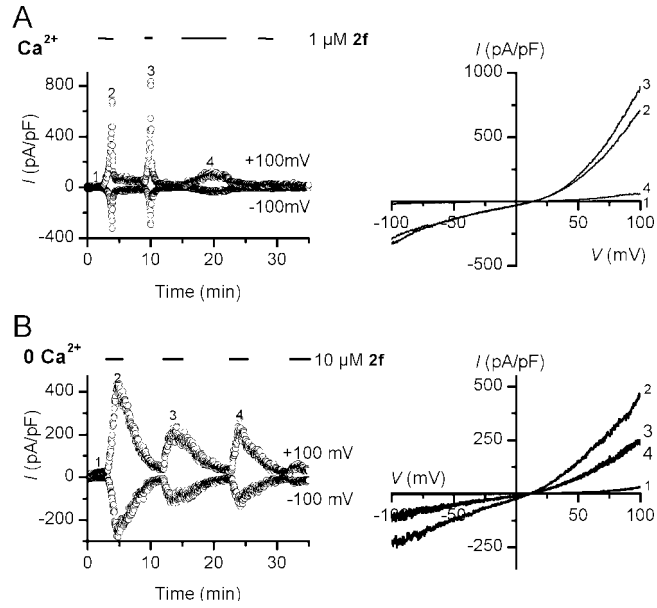

Figure 5. Characteristics currents activated by **2f**. Whole cell currents were analyzed in mTRPV4-transfected HEK293 cells as described in the Experimental Section. (A) Left: Whole cell mTRPV4 current development as a function of time. In Ca^{2+} containing solutions, currents in mTRPV4 transfected cells were monitored via ramp protocols from −100 mV to +100 mV. Compound **2f** was included in the extracellular solution as indicated by the top bar. The traces are representative of five individual cells in >2 transfections. Right: I/V relationship of the **2f** activated currents. Same experiments as in Figure 4A. The numbers refer to ramps obtained at the times indicated by numbers in left panel. (B) Left: Experiment as in A, except for the absence of Ca^{2+} in the intra- and extracellular solutions. The traces are representative of five individual cells in >2 transfections. Right: I/V relationship of the **2f** activated currents in the absence of Ca^{2+}. Same experiments as in Figure 4C. The numbers refer to ramps indicated by numbers in Figure 4C.

in the same pocket as **2a** (Figure 5). Y556 is part of a YS motif in TM3, similar to that shown to be important for capsaicin activation of TRPV1.[20] On the other hand, while the residue TRPV1 equivalent (S512) to S557 in TRPV4 is important for binding of capsaicin to TRPV1,[20] its mutation to alanine had little effect on 4α-PDD binding to TRPV4 (Table 1).[21] Notably, the S557A mutation shifted the dose−response curve for activation of TRPV4 by **2f** toward higher concentrations. Although this shift was less pronounced than in the Y556A mutant (Figure 6), it suggests that the increased potency of **2f** compared to **2a** may be related to the presence of a further binding element in TRPV4 for **2f**. Because serine is a polar element, it is unlikely that this residue directly interacts with the acyl moiety of **2f**, supporting the view that, compared to other side chains, the hexanoate moiety positions the polar diterpenoid core in a more optimal orientation for interaction with TRPV4 rather than directly interacting with the binding site. The involvement of both Y556 and S557 in TRPV4 gating is reminiscent of similar observations reported for TRPV1[20] and suggests that these two channels share similar gating properties.

Changes to the A,B Ring Junction. The A,B ring junction is a critical structural feature of the phorboid TRPV4 pharmacophore. To further explore this dependence, 4α-PDD (**2a**) was subjected to photocyclization, generating its corresponding cage-like lumiphorbol derivative (**5**), while the 4-deoxygenated 4α-PDD analogue (**4c**) was prepared from 4α-4-deoxphorbol (**4b**). Compound **4c** was unable to activate TRPV4 (Table 1), suggesting that the 4-hydroxyl is crucial for agonist activation of TRPV4. Conversely, 4α-LPDD (**5**) outperformed 4α-PDD (**2a**) in terms of TRPV4 activation, with an almost 2-fold lower EC_{50} value (175 ± 0.07 vs 370 nM, Table 1 and Figure 7A for **5**). At 0.1 μM concentration, **5** could still elicit a significantly greater increase in $[Ca^{2+}]_i$ in mTRPV4 transfected HEK293 cells than did **2a** (data not

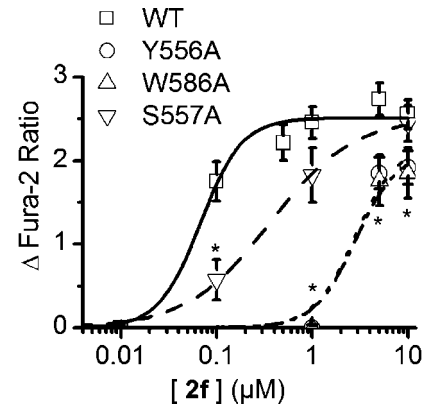

Figure 6. (D) Dose−response relationship for **2f** in TM3-4 mTRPV4 mutants. Dose−response relationship for **2f** in mTRPV4 mutants. HEK293 cells were transiently transfected with either wild type mTRPV4 (WT, square symbols), or the mutants Y556A (circles), S557A (downward triangles), or W586A (upward triangles). Agonist activity of **2f** was tested by Ca^{2+} imaging as described in the Experimental Section, and shown as ΔFura-2 ratio. Data for each point are calculated from >16 individual cells from three independent transfections. * indicates significant differences from wild type (p < 0.05).

shown, p < 0.01). On the other hand, at concentrations above 10 μM, **5** elicited $[Ca^{2+}]_i$ responses also in nontransfected cells (not shown). These $[Ca^{2+}]_i$ responses were not increased by the expression of TRPV1−3, indicating that 4α-LPDD (**5**) did not affect related TRP channels (data not shown). However, at less than 10 μM, there was no effect of **5** in

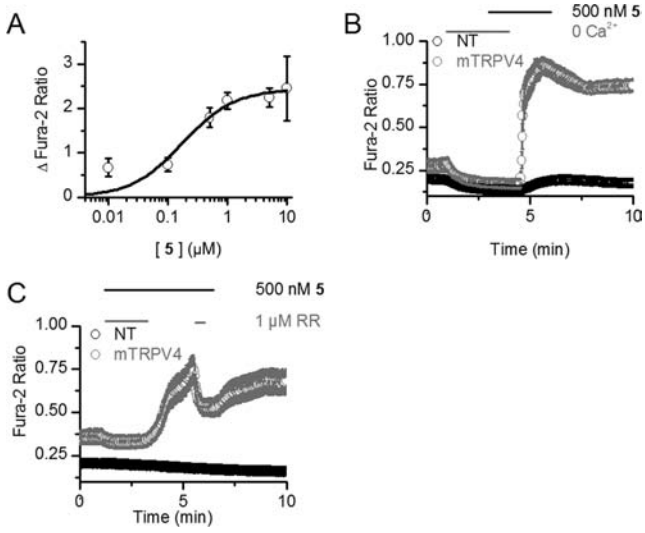

Figure 7. Effects of 4α-LPDD (5) on $[Ca^{2+}]_i$ in mTRPV4 transfected HEK 293 cells. (A) Dose−response relationship for **5**. ΔFura-2 ratio was estimated by single cell Ca^{2+} imaging as described in the Experimental Section. Points are ΔFura-2 ratio estimated for 24−71 individual cells from three independent transfections. The solid line represents a fit to the Hill equation. (B) The response to **5** is dependent on extracellular Ca^2. Compound **5** (500 nM) and extracellular Ca^{2+} were present as indicated by the top bars. The figure is representative of three independent experiments. (C) The $[Ca^{2+}]_i$ response to **5** (500 nM) is inhibited by ruthenium red (RR, 1 μM). The presence of RR and **5** in the extracellular solution is indicated by the bars. The figure is representative of three independent experiments.

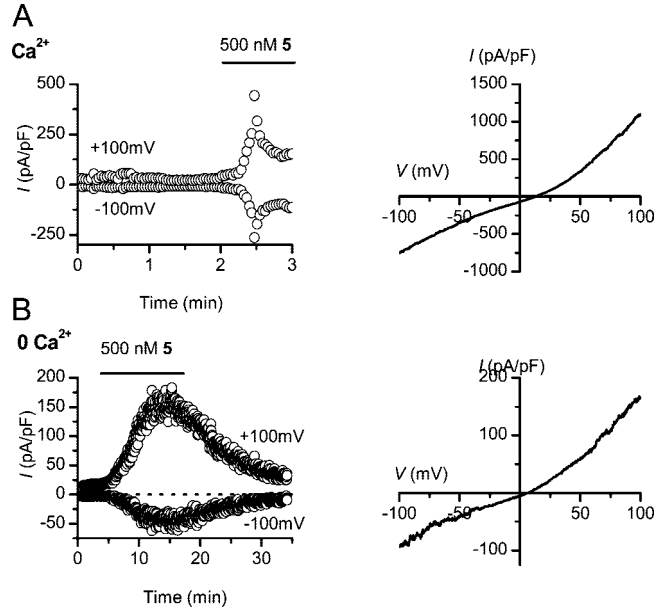

Figure 8. Characteristics of currents activated by 4α-LPDD (**5**). Whole cell currents were analyzed in mTRPV4-transfected HEK293 cells as described in the Experimental Section. (A) Left: Whole cell mTRPV4 current development as a function of time. In Ca^{2+} containing solutions, currents in mTRPV4-transfected cells were monitored via ramp protocols from −100 mV to +100 mV. Compound **5** was included in the extracellular solution as indicated by the bar. The figure is representative of five individual cells from >2 transfections. Right: I/V relationship for currents activated by **5**. Same experiment as in Figure 7A. (B) Left: Conditions as in A, except that the experiment was carried out in the absence of Ca^{2+} in both the intra- and extracellular solutions. Note the dramatic difference in current duration. The figure is representative of five individual cells from >2 transfections. Right: I/V relationship for currents activated by **5** in the absence of Ca^{2+}. Same experiment as in Figure 7C.

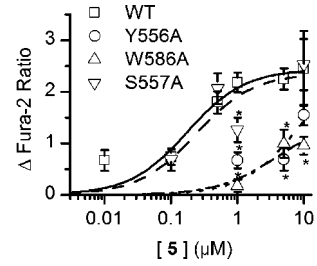

Figure 9. Dose−response relationship for 4α-LPDD (**5**) in TM3-4 mTRPV4 mutants: Dose−response relationship for the $[Ca^{2+}]_i$ response elicited by **5** in HEK 293 cells transfected with wild type mTRPV4 (WT, square symbols), or the mutants Y556A (circles), S557A (downward triangles), or W586A (upward triangles). The agonist activity of **2f** was tested by Ca^{2+} imaging as described in the Experimental Section and shown as ΔFura-2 ratio. Data for each point are calculated from $n > 15$ individual cells from three independent transfections. * indicates significant differences from WT ($p < 0.05$).

nontransfected cells, neither in Ca^{2+} imaging experiments (Figure 7B,C) nor in patch clamp studies (data not shown). Furthermore, the $[Ca^{2+}]_i$ response to **5** was dependent on extracellular Ca^{2+} and was inhibited by RR (Figure 7B,C), strongly suggesting that it reflects activation of TRPV4.

In patch clamp studies, **5** activated typical TRPV4 outward−inward rectifying currents in both the presence (Figure 7A) and in the absence (Figure 8B) of extra- and intracellular Ca^{2+}. A number of significant differences between the TRPV4 currents triggered by the 4α-lumiphorbol ester (**5**) and by 4α-phorbol esters (**2a** and **2f**) were observed. Most notably, the same current densities were observed irrespective of the presence of Ca^{2+} in recording solutions (Ca^{2+} vs no Ca^{2+}; 505 ± 102 pA/pF vs 635 ± 107 pA/pF; $p > 0.4$ at 100 mV, $n = 5-6$). This is in contrast to 4α-PDD (**2a**), where Ca^{2+}-dependent potentiation of TRPV4 is well described[27,28] and to currents activated by 4α-PDH (**2f**) (Ca^{2+} vs no Ca^{2+}; 354 ± 112 pA/pF vs 806 ± 132 pA/pF; $p < 0.05$ at 100 mV, $n = 6-7$) Second, in contrast to the transient current activation by 4α-phorbol esters (Figure 5), currents activated by the lumiphorbol (**5**) were maintained in Ca^{2+} free solutions (Figure 8B). Hence, currents activated by 4α-PDH (**2f**) inactivated with an initial slope of −16.5 ± 4.9% min^{-1}, while the 4α-LPDD (**5**) had an almost constant slope of 1.0 ± 1.0% min^{-1} after activation that was significantly different ($P = 0.018$, $n = 4-5$). These findings highlight the critical role for the ring A,B-junction for functional agonist activity.

To gain information on the requirements for binding of **5** to TRPV4, dose−response experiments for the 4α-LPDD-induced increase in $[Ca^{2+}]_i$ were carried out on wild type TRPV4 and on W586A, S557A, and Y556A mutant TRPV4. The W586A and Y556A mutations resulted in rightward shifts of the dose−response curve (Figure 9), whereas the S557A mutation had no effect. These observations are in agreement with previously published results for 4α-PDD (**2a**)[21] (Table 1). Because **2a** differs from **5** in the headgroup and from **2f** only in the length of the acyl groups, the fact that the S557A mutation attenuates binding of **2f** but not of **2a** and **5** must be related to the acyl decoration of the terpenoid core, seemingly due to a suboptimal orientation of the terpenoid core with S557. Because 4α-PDD (**2a**) and its lumiphorbol derivative (**5**) apparently bind the same pocket of TRPV4, the substantially different features of the currents elicited by these ligands suggest, in fact, that

their terpenoid cores interact in a different way with the ligand binding site of the receptor.

Conclusions

We have provided evidence that 4α-phorbol esters are useful tools to investigate the mechanism of activation of TRPV4 by small molecules. Our findings strongly indicate that the lipophilic side chains on the C-ring, although critical for TRPV4 activation, serve mainly as a steering element for a correct positioning of the terpenoid core into the phorboid binding pocket of TRPV4, where a critical role has been identified for the TM3 YS motif. Moreover, we have demonstrated that the nature of the A,B ring junction plays a major role in binding of 4α-phorbol esters to TRPV4. Finally, the marked difference between 4α-phorbol- and 4α-lumiphorbol derivatives in their effects on TRPV4 activity imply the existence of multiple mechanisms to translate affinity into functional activity for this class of compounds. In this context, the possibility of producing continuous rather than transient TRPV4 activation could has major implications for the therapeutic exploitation of TRPV4 agonists (e.g., bladder dysfunction[14,28]). Taken together, these results illustrate the potential of combining structure−activity studies and site-directed mutagenesis to map binding pockets of "difficult" proteins, providing information useful to design synthetic small molecule agonists for these proteins.

Experimental Section

Materials. Gravity column chromatography: Merck silica gel (70−230 mesh). IR: Shimadzu DR 8001 spectrophotometer. NMR: Jeol Eclipse (300 and 75 MHz for ^{1}H and ^{13}C, respectively). For ^{1}H NMR, $CDCl_3$ as solvent, $CHCl_3$ at $\delta = 7.26$ as reference. For ^{13}C NMR, $CDCl_3$ as solvent, $CDCl_3$ at $\delta = 77.0$ as reference. Commercial dry CH_2Cl_2 and THF were filtered from neutral alumina before use. Reactions were monitored by TLC on Merck 60 F_{254} (0.25 mm) plates that were visualized by UV inspection and/or staining with 5% H_2SO_4 in ethanol and heating. Organic phases were dried with Na_2SO_4 before evaporation. A Beckmann apparatus equipped with a UV detector set at 254 nm (refraction index for **5**) was used to assess purity (>95%) of all final products. A LUNA SI60 column was used, with isocratic elution with MeOH−H_2O 4:1, and 2.0 mL/min as flow rate. R_t ranged from 17 min (**2c**) to 34 min (**2j**).

Synthesis of 4α-Phorbol Diesters (2e−j) and the 4α-4-Deoxyphorbol Diester (4c): Synthesis of 4α-PDH (2f) as Representative for the Process. To a solution of 4α-phorbol (**2d**, 500 mg, 1.37 mmol) in CH_2Cl_2−THF (1:1, 10 mL), hexanoic acid (858 μL, 6.71 mmol, 5 mol equiv), EDC (1.58 g, 8.12 mmol, 6 mol equiv), and DMAP (251 mg, 2.1 mmol, 1.5 mol equiv) were added. After stirring at room temperature for 4 h, the reaction was worked up by the addition of brine and extraction with CH_2Cl_2. The organic phase was filtered over neutral alumina (5 g) to remove unreacted hexanoic acid, and the filtrate was evaporated to afford 870 mg of crude 4α-phorbol 12,13,20-trihexanoate. The latter was dissolved in methanol (7 mL), and the solution was brought to pH 2 by the addition of few drops of 65% $HClO_4$. After stirring overnight at room temperature, the reaction was worked up by the addition of solid $NaHCO_3$, filtration, and evaporation. The residue was purified by gravity column chromatography on silica gel (13 g, petroleum ether−EtOAc 7:3 as eluant) to afford 245 mg (30% from 4α-phorbol) (**2f**) as a colorless oil.

Synthesis of the 4α-Phorbol Monoester (2k). To a solution of 4α-phorbol (**2d**, 200 mg, 0.55 mmol) in CH_2Cl_2−THF (1:1, 10 mL), decanoic (capric) acid (284 mg, 1.65 mmol, 3 mol equiv), EDC (370 mg, 1.93 mmol, 3.5 mol equiv), and DMAP (67 mg, 0.55 mmol, 1 mol equiv) were added. After stirring at room temperature for 2 h, the reaction was worked up by the addition of brine and extraction with CH_2Cl_2. The organic phase was filtered over neutral alumina (2 g) to remove unreacted decanoic acid, and the filtrate was evaporated to afford 870 mg of crude 4α-phorbol 12,20-didecanoate. The latter was dissolved in methanol (7 mL), and the solution was brought to pH 2 by the addition of few drops of 65% $HClO_4$. After stirring overnight at room temperature, the reaction was worked up by the addition of solid $NaHCO_3$, filtration, and evaporation. The residue was purified by gravity column chromatography on silica gel (6 g, petroleum ether-EtOAc 7:3 as eluant) to afford 48 mg (13% from 4α-phorbol) **2k** as a colorless oil.

Synthesis of LUMI 4α-PDD (5). A solution of 4α-PDD (**2a**) in ethanol was degassed in a flow of nitrogen for 40 min and then irradiated in an immersion well photoreactor with a low-pressure mercury lamp. After 24 h of irradiation, the reaction was evaporated and the residue was purified by gravity column chromatography on silica gel (5 g, petroleum ether−EtOAc 8:2 as eluant) to afford 190 mg (95%) **5** as a colorless oil.

Cell Culture and Transfection. Human embryonic kidney cells, HEK293, were grown in DMEM containing 10% human serum, 2 mM L-glutamine, 2 units/mL penicillin and 2 mg/mL streptomycin, in a 37 °C/10% CO_2 incubator. Transient transfection of HEK293 cells with mTRPV4 (accession number Q9EPK8) in the pCAGGS/Ires-GFP vector[29] was performed using Mirus TransIT-293 transfection agent (Mirus Corporation; Madison, WI) and cells where incubated overnight before experiments. For both $[Ca^{2+}]_i$ measurements and electrophysiological experiements, the cells were trypsinized and seeded on poly-L-lysine coated coverslips on the day of the experiment. The mTRPV4 expressing cells were identified by GFP expression. GFP-negative cells from the same coverslips were used as untransfected controls.

Solutions. For $[Ca^{2+}]_i$ measurements, cells were constantly perfused with Krebs solution containing (in mM): 150 NaCl, 6 KCl, 1 $MgCl_2$, 1.5 $CaCl_2$, 10 HEPES, 10 glucose, pH 7.4. Where indicated, $CaCl_2$ was emitted from the solution. For electrophysiological studies, the extracellular solution contained (in mM): 150 NaCl, 6 CsCl, 1 $MgCl_2$, 5 $CaCl_2$, 10 glucose, and 10 HEPES, pH 7.4. For Ca^{2+} free experiments, $CaCl_2$ was omitted from the solution. The pipet solution contained (in mM): 20 CsCl, 100 aspartate, 1 $MgCl_2$, 10 HEPES, 4 Na-ATP, 10 K-1,2-bis(2-aminophenoxy)ethane *N*,*N*,*N*′,*N*′-tetraacetate (BAPTA), pH 7.4. Ca^{2+} was buffered to a free concentration of 200 nM with $CaCl_2$ as calculated using the software CaBuf (G. Droogmans) or omitted for Ca^{2+} free pipet solutions.

Electrophysiological Recording. All electrophysiological data were obtained using 400 ms linear ramp protocols between −100 mV and 100 mV after a 50 ms prepulse at −100 mV as previously described.[19] Ramps were performed every 2 s, and the cells were kept at a holding potential of −30 mV between ramps. Data were recorded with 2 kHz sample rate using an EPC10 amplifier controlled by PatchMaster software (Heka, Lambrecht, Germany) and filtered at 2.9 kHz using the built-in Bessel filter. Pipets had resistances of 2−4 MΩ in asymmetrical recording solutions and an Ag-AgCl wire was used as reference electrode. Capacitance and 70−80% of the series resistance were electronically compensated.

$[Ca^{2+}]_i$ Measurements. Cells were preincubated for 30 min at 37 °C with 4 μM Fura-2 AM (TefLab, Austin, TX) in normal growth medium and mounted on the stage of an IX81 inverted microscope (Olympus, Tokyo, Japan). The imaging system consisted of a MT10 filter-based illumination system (Olympus) and a CCD Camera (Olympus). Illumination and imaging was controlled by CellM software (Olympus). $[Ca^{2+}]_i$ was estimated as the ratio of the emitted fluorescence at 510 nm after excitation at 340 and 380 nm, respectively (fura-2 ratio). The background fluorescence was digitally subtracted from individual experiments before the ratio was calculated.

Data Analysis and Statistics. Electrophysiological data where analyzed using Patchmaster software (HEKA, Lambrecht, Germany), WinACD (Guy Drogmans, ftp://ftp.cc.kuleuven.ac.be/pub/droogmans/winascd.zip) and Origin (OrigineLab, Northampton, MA). Fura-2 AM fluorescence ratios were calculated in CellM Software (Olympus) and Origin (OrigineLab, Northampton, MA).

ΔFura-2 ratio was calculated as $(R_t - R_{t=0})/R_{t=0}$, and maximal response plus time of maximal response were analyzed for individual cells. EC_{50} values were calculated using the Hill equation:

$$R_{max} = V_{max}\frac{C^n}{EC_{50}^n + C^n} \quad (1)$$

where R_{max} is the maximal ratio at the given concentration (C), V_{max} is the maximal response, n is the Hill coefficient, and EC_{50} denotes the concentration eliciting half-maximal response.

Data are summarized as mean ± standard error of the mean (SEM). Individual experiments shown are representative of at least three independent experiments.

Acknowledgment. We thank all the members of the Ion Channel Research Laboratory at the KU Leuven for helpful discussions. This work was supported by grants from Interuniversity Attraction Poles Program−Belgian State−Belgian Science Policy (P6/28), the Research Council of the KU Leuven (GOA 2004/07), and the Flemish Government (Excellentiefinanciering, EF/95/010, to B.N.), by Danish Natural Sciences Research Foundation (E.K.H. and S.F.P.), the Gangsted Foundation (S.F.P.), and the Lundbeck Foundation (E.K.H.).

Supporting Information Available: Full spectroscopic data for all final products. This material is available free of charge via the Internet at http://pubs.acs.org.

References

(1) Pedersen, S. F.; Owsianik, G.; Nilius, B. TRP Channels: an Overview. *Cell Calcium* **2005**, *38*, 233–252.
(2) Owsianik, G.; D'Hoedt, D.; Voets, T.; Nilius, B. Structure−Function Relationship of the TRP Channel Superfamily. *Rev. Physiol. Biochem. Pharmacol.* **2006**, *156*, 61–90.
(3) Voets, T.; Talavera, K.; Owsianik, G.; Nilius, B. Sensing with TRP Channels. *Nat. Biol. Chem.* **2005**, *1*, 85–92.
(4) Montell, C. The TRP Superfamily of Cation Channels. *Sci. STKE* **2005**, *2005*, re3.
(5) Venkatachalam, K.; Montell, C. TRP Channels. *Annu. Rev. Biochem.* **2007**, *76*, 387–417.
(6) Jordt, S. E.; Ehrlich, B. E. TRP Channels in Disease. *Subcell. Biochem.* **2007**, *45*, 253–271.
(7) Appendino, G.; Szallasi, A. Clinically Useful Vanilloid Receptor TRPV1 Antagonists: Just Around the Corner (or Too Early to Tell)? *Prog. Med. Chem.* **2006**, *44*, 145–180.
(8) Appendino, G.; Minassi, A.; Pagani, A.; Ech-Chahad, A. The Role of Natural Products in the Ligand Deorphanization of TRP Channels. *Curr. Pharm. Des.* **2008**, *14*, 2–17.
(9) Vennekens, R.; Owsianik, G.; Nilius, B. Vanilloid Transient Receptor Potential Cation Channels: An Overview. *Curr. Pharm. Des.* **2008**, *14*, 18–31.
(10) Nilius, B.; Owsianik, G.; Voets, T.; Peters, J. A. Transient Receptor Potential Channels in Disease. *Physiol. Rev.* **2007**, *87*, 165–217.
(11) Smith, P. L.; Maloney, K. N.; Pothen, R. G.; Clardy, J.; Clapham, D. E. Bisandrographolide from *Andrographis Paniculata* Activates TRPV4 Channels. *J. Biol. Chem.* **2006**, *281*, 29897–29904.
(12) Watanabe, H.; Davis, J. B.; Smart, D.; Jerman, J. C.; Smith, G. D.; Hayes, P.; Vriens, J.; Cairns, W.; Wissenbach, U.; Prenen, J.; Flockerzi, V.; Droogmans, G.; Benham, C. D.; Nilius, B. Activation of TRPV4 Channels (hVRL-2/mTRP12) by Phorbol Derivatives. *J. Biol. Chem.* **2002**, *277*, 13569–13577.
(13) Vriens, J.; Owsianik, G.; Janssens, A.; Voets, T.; Nilius, B. Determinants of 4α-Phorbol Sensitivity in Transmembrane Domains 3 and 4 of the Cation Channel TRPV4. *J. Biol. Chem.* **2007**, *282*, 12796–12803.
(14) Thorneloe, K. S.; Sulpizio, A. C.; Lin, Z.; Figueroa, D. J.; Clouse, A. K.; McCafferty, G. P.; Chendrimada, T. P.; Lashinger, E. S.; Gordon, E. A.; Evans, L.; Misajet, B. A.; Demarini, D. J.; Nation, J. H.; Casillas, L. N.; Marquis, R. W.; Votta, B. J.; Sheardown, S. A.; Xu, X.; Brooks, D. P.; Laping, N.; Westfall, T. D. GSK1016790A, a Novel and Potent TRPV4 Channel Agonist Induces Urinary Bladder Contraction and Hyperactivity: Part I. *J. Pharmacol. Exp. Ther.* **2008**, *326*, 432–442.
(15) Willette, R.; Bao, W.; Nerurkar, S.; Yue, T. L.; Doe, C. P.; Stankus, G.; Turner, G. H.; Ju, H.; Thomas, H.; Fishman, C.; Sulpizio, A.; Behm, D.; Hoffman, S.; Lin, Z.; Lozinskaya, I.; Casillas, L.; Lin, M.; Trout, R. E. T.; Thorneloe, K.; Lashinger, E. S.; Figueroa, D. J.; Votta, B.; Marquis, R.; Xu, X. Systemic Activation of the Transient Receptor Potential V4 Channel Causes Endothelial Failure and Circulatory Collapse: Part 2. *J. Pharmacol. Exp. Ther.* **2008**, *326*, 443–452.
(16) Goel, G.; Makkar, H. P.; Francis, G.; Becker, K. Phorbol Esters: Structure, Biological Activity, and Toxicity in Animals. *Int. J. Toxicol.* **2007**, *26*, 279–288.
(17) Rios, M. Y.; Aguilar-Guadarrama, A. B. Nitrogen-Containing Phorbol Esters from *Croton ciliatoglandulifer* and their Effects on Cyclooxygenases-1 and -2. *J. Nat. Prod.* **2006**, *69*, 887–890.
(18) Gavva, N. R.; Klionsky, L.; Qu, Y.; Shi, L.; Tamir, R.; Edenson, S.; Zhang, T. J.; Viswanadhan, V. N.; Toth, A.; Pearce, L. V.; Vanderah, T. W.; Porreca, F.; Blumberg, P. M.; Lile, J.; Sun, Y.; Wild, K.; Louis, J. C.; Treanor, J. J. Molecular Determinants of Vanilloid Sensitivity in TRPV1. *J. Biol. Chem.* **2004**, *279*, 20283–20295.
(19) Vriens, J.; Owsianik, G.; Janssens, A.; Voets, T.; Nilius, B. Determinants of 4α-Phorbol Sensitivity in Transmembrane Domains 3 and 4 of the Cation Channel TRPV4. *J. Biol. Chem.* **2007**, *282*, 12796–12803.
(20) Jordt, S. E.; Julius, D. Molecular Basis for Species-Specific Sensitivity to "Hot" Chili Peppers. *Cell* **2002**, *108*, 421–430.
(21) Vriens, J.; Watanabe, H.; Janssens, A.; Droogmans, G.; Voets, T.; Nilius, B. Cell Swelling, Heat, and Chemical Agonists Use Distinct Pathways for the Activation of the Cation Channel TRPV4. *Proc. Natl. Acad. Sci. U.S.A* **2004**, *101*, 396–401.
(22) Appendino, G.; Bertolino, A.; Minassi, A.; Annunziata, R.; Szallasi, A.; De Petrocellis, L.; Di Marzo, V. Synthesis and Biological Evaluation of Phorbol−Resiniferatoxin RTX) Hybrids. *Eur. J. Org. Chem.* **2004**, 3413−3421.
(23) Appendino, G.; Carello, G. P.; Enriù, R.; Jakupovic, J. A New Rearrangement of a Phorbol Derivative. *J. Nat. Prod.* **1995**, *58*, 284–287.
(24) Marquez, N.; Calzado, M. A.; Sanchez-Duffhues, G.; Perez, M.; Minassi, A.; Appendino, G.; Diaz, L.; Muñoz-Fernández, A. A.; Muñoz, E. Differential Effects of Phorbol-13-Monoesters on Human Immunodeficiency Virus Reactivation. *Biochem. Pharmacol.* **2008**, *75*, 1370–1380.
(25) Appendino, G. Capsaicin and Capsainoids. In *Modern Alkaloids: Structure Isolation, Synthesis, and Biology*; Fattorusso, E., Taglialatela-Scafati, O., Eds.; Wiley: Weinheim, 2007; pp 75−112.
(26) Appendino, G.; Minassi, A.; Morello, A. S.; De Petrocellis, L.; Di Marzo, V. *N*-Acylvanillamides: Development of an Expeditious Synthesis and Discovery of New Acyl Templates for Powerful Activation of the Vanilloid Receptor. *J. Med. Chem.* **2002**, *45*, 3739–3745.
(27) Strotmann, R.; Schultz, G.; Plant, T. D. Ca^{2+}-Dependent Potentiation of the Nonselective Cation Channel TRPV4 Is Mediated by a C-Terminal Calmodulin Binding Site. *J. Biol. Chem.* **2003**, *278*, 26541–26549.
(28) Gevaert, T.; Vriens, J.; Segal, A.; Everaerts, W.; Roskams, T.; Talavera, K.; Owsianik, G.; Liedtke, W.; Daelemans, D.; Dewachter, I.; Van Leuven, F.; Voets, T.; De Ridder, D.; Nilius, B. Deletion of the Transient Receptor Potential Cation Channel TRPV4 Impairs Murine Bladder Voiding. *J. Clin. Invest.* **2007**, *117*, 3453–3462.
(29) Nilius, B.; Prenen, J.; Wissenbach, U.; Bödding, M.; Droogmans, G. Differential Activation of the Volume-Sensitive Cation Channel TRP12 (OTRPC4) and Volume-Regulated Anion Currents in HEK-293 Cells. *Pflügers Arch.* **2001**, *443*, 227–233.

JM9001007